複数点の海洋汚染物質の海中漏出位置推定法の開発

課題責任者
佐藤　徹　　東京大学 大学院新領域創生科学研究科　海洋技術環境学専攻

著者
金尾 俊介*[1], 佐藤 徹*[1], 山口 アラン 純二*[1]
*[1] 東京大学 大学院新領域創生科学研究科　海洋技術環境学専攻

海洋で異常に高い濃度の汚染物質が観察された場合、汚染物質の漏れ位置とフラックスを検索する必要がある。この研究では、このような検出作業の時間と費用を削減するために、観測された限られた数の濃度データを使用して、複数の漏れ位置とフラックスを推定する数値手法を提案する。この方法は adjoint marginal sensitivity method と呼ばれ、漏れの位置とフラックスを推定するための逆方向時間の確率的方法です。提案手法の新規性として、複数の漏洩点に対応できることがあげられる。本研究では、新しく開発された手法を検証し、流れの速度、2 点の漏出位置間の距離、および空間観測範囲につき、一連の二次元のケーススタディのシミュレーションを実施し、それらの推定精度に対する影響を調べた。

キーワード：アジョイント法; 海洋流体力学; 限界感度法; 海洋汚染物質; 複数漏出位置の推定

1. 序論

地球温暖化の抑制のため，大気への CO_2 排出量削減が必要とされる中，CO_2 を発電所や工場などの排出源で分離・回収し海底下の貯留層に圧入・貯蔵する海底下 CCS (CO_2 Capture and Storage) が注目されている．海中への CO_2 漏出の可能性を考慮し，海洋汚染防止法により，海底下 CCS 事業者は海中 CO_2 濃度の監視が義務付けられている．その際に高濃度が検出された場合に再調査を行なう必要があるが，それは多額の費用と長い時間を要する．そこで，観測濃度データを用いつつ漏出位置を数値的に推定することで，再調査の範囲を絞り，その費用と所要時間を削減することが求められる．

海底下 CCS で想定される，非定常な流れの下での漏出位置・時刻・量の全ての推定に関する先行研究としては，Adjoint Marginal Sensitivity Method を適用した森ら[1]や Sakaizawa et al. [2]があるが，1 点からの漏出しか考慮されていない．実際は 1 点漏出とは限らないため，本研究では，複数点からの漏出を推定できる手法の開発，および本手法の使用に際しての知見と適用限界を示すことを目的とする．

2. 手法

2.1 順時間方向計算

流速データを得るために，ここでは静水圧近似の下での Navier-Stokes 方程式(1)〜(3)と連続の式(4)を解く．ただし t は時刻，u, v, w は x, y, z 方向の流速，p は圧力，ρ, ρ_0 は密度および基準密度，A_M, K_M は水平・鉛直方向の渦粘性係数，g は重力加速度，f_{Cor} はコリオリパラメタである．

$$\frac{\partial u}{\partial t}+u\frac{\partial u}{\partial x}+v\frac{\partial u}{\partial y}+w\frac{\partial u}{\partial z}-f_{cor}v$$

$$=-\frac{1}{\rho_0}\frac{\partial p}{\partial x}+A_{\mathrm{M}}\left(\frac{\partial^2 u}{\partial x^2}+\frac{\partial^2 u}{\partial y^2}\right)+\frac{\partial}{\partial z}\left(K_{\mathrm{M}}\frac{\partial u}{\partial z}\right) \qquad (1)$$

$$\frac{\partial v}{\partial t}+u\frac{\partial v}{\partial x}+v\frac{\partial v}{\partial y}+w\frac{\partial v}{\partial z}+f_{cor}u$$

$$=-\frac{1}{\rho_0}\frac{\partial p}{\partial y}+A_{\mathrm{M}}\left(\frac{\partial^2 v}{\partial x^2}+\frac{\partial^2 v}{\partial y^2}\right)+\frac{\partial}{\partial z}\left(K_{\mathrm{M}}\frac{\partial v}{\partial z}\right) \qquad (2)$$

$$0=-\frac{1}{\rho_0}\frac{\partial p}{\partial z}-\frac{\rho}{\rho_0}g \qquad (3)$$

$$\frac{\partial u}{\partial x}+\frac{\partial v}{\partial y}+\frac{\partial w}{\partial z}=0 \qquad (4)$$

本研究では，本手法の有効性および使用法を調べるため，計算上で CO_2 を漏出・移流拡散させ，それを推定する．式(5)の C は CO_2 濃度，S_C は漏出項，A_C, K_C は水平・鉛直方向の渦拡散係数である．

$$\frac{\partial C}{\partial t}+\frac{\partial(u_j C)}{\partial x_j}=\frac{\partial}{\partial x_j}\left(D_C\frac{\partial C}{\partial x_j}\right)+S_C+q_{\mathrm{in}}C_{\mathrm{in}}-q_{\mathrm{out}}C \qquad (5)$$

2.2 逆時間方向計算

本研究で適用する Adjoint Marginal Sensitivity Method では，保存した流速データを用いつつ，逆時間方向に adjoint probability ψn (n = 1, ..., N) を移流拡散させる．ここで N は観測データの個数である．

$$\frac{\partial \psi^*}{\partial \tau}-u_j\frac{\partial \psi^*}{\partial x_j}=\frac{\partial}{\partial x_j}\left(D_C\frac{\partial \psi^*}{\partial x_j}\right)-q_{\mathrm{out}}\psi^*$$

$$+\Pi(\boldsymbol{x}-\boldsymbol{x}_{\mathrm{obs}})\Pi'(\tau\,;\,\tau_{\mathrm{obs}}-\Delta\tau_{\mathrm{obs}}\,,\tau_{\mathrm{obs}}) \qquad (6)$$

ここで τ は逆時刻，$x_{obs, n}, \tau_{obs, n}$ は各観測の位置と逆時刻で，$\Pi(\boldsymbol{x})$ は $\boldsymbol{x}=0$ のとき 1 を，$\boldsymbol{x}\neq 0$ のとき 0 をとる矩形関数である．なお adjoint probability は時間の次元をもつ．1 点漏出の CO_2 体積フラックス f は

$$\bar{f}=\frac{\sum G_n\Psi_n}{\sum {\Psi_n}^2} \qquad (7)$$

$$G_n = \int_{t_{\mathrm{obs},n}}^{t_{\mathrm{obs},n}+\Delta t_{\mathrm{obs},n}} C_n\left(\boldsymbol{x}_{\mathrm{obs},n}, t\right) \mathrm{d}t \qquad (8)$$

$$\Psi_n = \frac{|\Delta \boldsymbol{x}_{\mathrm{seep}}|}{|\Delta \boldsymbol{x}_{\mathrm{obs},n}|} \int_{\tau_{\mathrm{seep}}-\Delta\tau_{\mathrm{seep}}}^{\tau_{\mathrm{seep}}} \psi_n^*\left(\boldsymbol{x}_{\mathrm{seep}}, \tau\right) \mathrm{d}\tau \qquad (9)$$

と推定される．ただしfは一定値であり，C_nは各観測濃度，Δtは計算時間増分，x_{seep}は漏出位置で，τ_{seep}, $\Delta\tau$seepは漏出開始逆時刻，漏出継続時間である．連続CO_2漏出の場合は$\tau_{seep} - \Delta\tau_{seep} = 0$とする．

複数点漏出の場合は，CO_2濃度に関する重ね合わせの原理より，観測濃度C_nを漏出点 A, B 由来の到達濃度C_{An}, C_{Bn}に分解し，各漏出フラックスf_A, f_Bを同様に推定する．到達濃度は未知なので消去して，

$$\Psi_{NA} f_A + \Psi_{NB} f_B = G_N \qquad (10)$$

を導出する．ここでΨ_{nA}, Ψ_{nB}は漏出点 A, B でψ_nを時間積分した値である．この連立方程式の最小 2 乗解である推定漏出フラックスは式(11), (12)で表され，推定漏出位置・時刻は式(13)の指標 SDN2 を最小化する位置・時刻である．ただし，問題の単純化のため，CO_2が複数点から同時に漏出するものとした．

$$\bar{f}_A = \frac{(\sum G_n\Psi_{nA})(\sum {\Psi_{nB}}^2) - (\sum G_n\Psi_{nB})(\sum \Psi_{nA}\Psi_{nB})}{(\sum {\Psi_{nA}}^2)(\sum {\Psi_{nB}}^2) - (\sum \Psi_{nA}\Psi_{nB})^2} \qquad (11)$$

$$\bar{f}_B = \frac{(\sum G_n\Psi_{nB})(\sum {\Psi_{nA}}^2) - (\sum G_n\Psi_{nA})(\sum \Psi_{nA}\Psi_{nB})}{(\sum {\Psi_{nA}}^2)(\sum {\Psi_{nB}}^2) - (\sum \Psi_{nA}\Psi_{nB})^2} \qquad (12)$$

$$\mathrm{SDN2} = \frac{\sqrt{\frac{1}{N}\sum_{n=1}^{N}\{G_n - (\Psi_{nA}\bar{f}_A + \Psi_{nB}\bar{f}_B)\}^2}}{\frac{1}{N}\sum_{n=1}^{N} G_n}$$

$$= \frac{\sqrt{N\sum_{n=1}^{N}\{G_n - (\Psi_{nA}\bar{f}_A + \Psi_{nB}\bar{f}_B)\}^2}}{\sum_{n=1}^{N} G_n} \qquad (13)$$

3. 二次元テスト海域での 2 点漏出の推定結果

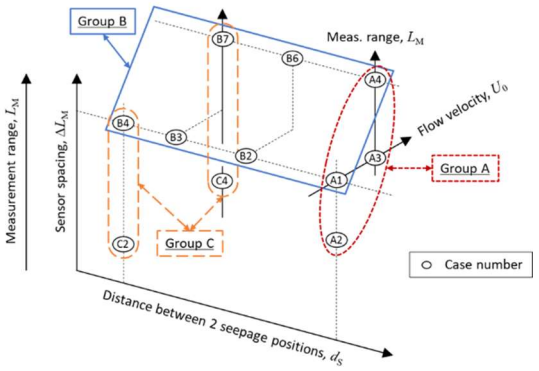

Fig. 1 Relationship among the cases for the two leakage point cases in Groups A, B, and C.

本研究では二次元テスト海域において，一様非定常流れの下でCO_2を順時刻t_{seep} = 51840 sec（逆時刻τ_{seep} = 120960 sec）から連続的に漏出させた．センサ個数を 16，渦拡散係数をD_C = 0.46 m²/s で固定し，センサ設置範囲の広さL_M（センサ間隔ΔL_M），移流長さ$L_A = U_0 T_p$ / π，2 漏出点間距離d_S，漏出フラックス比r，漏出位置とセンサ配置の Offset を変更しつつ推定した．Fig. 1 に各ケース間の関係を示す．Groups A～C ではr = 1 である．

一例として，Case A1 (U_0 = 0.2 m/s) での漏出位置，CO_2分布 (t = 120960 sec)，センサ配置を Fig. 2 に，Offset = 0 m のときの spatially min. SDN2 の時間変化を Fig. 3 に示す．真の漏出開始逆時刻付近で SDN2 が最小となった．以下 Re Sc = L_A^2 / (D_C T_p) を 10_2のオーダーの値とした場合の考察を記す．Group A で Offset = 0 m のときのL_M / L_Aと推定位置の誤差の関係を Fig. 4 に示す．Group A より，2 漏出位置の正確な推定には「L_M / L_Aが約 1.7 以上」が必要であることが分かる．

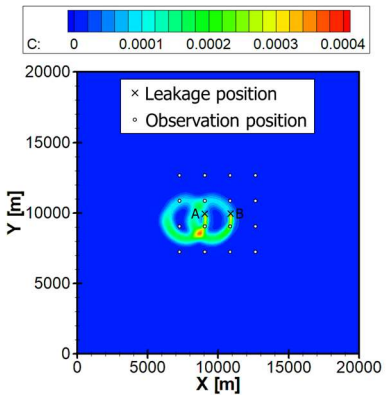

Fig. 2 Pollutant distribution at t = 129600 s and the observation positions in Case A1 for two leakage points.

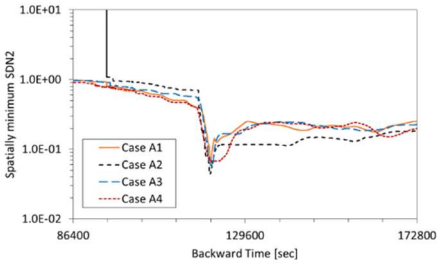

Fig. 3 Temporal change of the spatial minimum of SDN(2) in Group A for two leakage points.

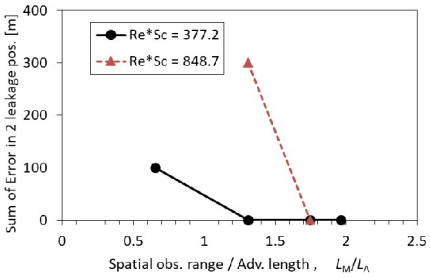

Fig. 4 Effect of nondimensional spatial observation range on estimated errors in leakage position in Group A for two leakage points.

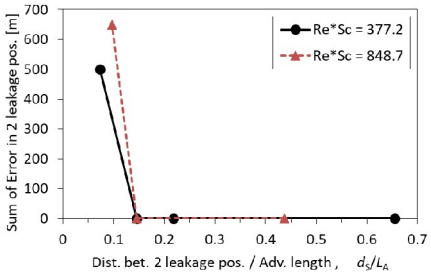

Fig. 5 Distance between two leakage positions and estimation error in them in Group B for two leakage points.

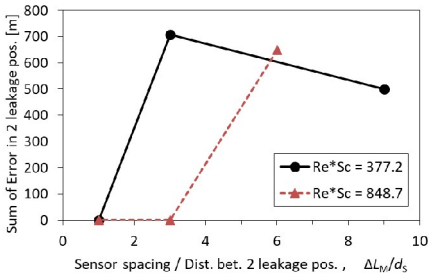

Fig. 6 Sensor spacing and estimation error in two leakage positions in Group C for two leakage points.

また Group B では Cases A1, A4 それぞれより d_S を短くした．Offset = 0 m のときの d_S / L_A と推定位置の誤差の関係を Fig. 5 に示す．Group A で示された条件は d_S / L_A が 0.15 以上で成り立つことが分かる．Group C では，d_S / L_A が 0.1 未満である Cases B2, B4 それぞれからセンサ間隔を短くした．Offset = 0 m のときの $\Delta L_M / d_S$ と推定位置の誤差の関係を Fig. 6 に示す．dS / LA が 0.15 以下の場合は「$\Delta L_M / d_S$ が 1 程度以下」が有効だと分かる．

4. 鹿児島湾を模擬した三次元テスト海域での連続 2 点漏出の推定

下島 [3] は鹿児島湾ハオリムシサイト東側斜面の頂上付近と麓の 2 箇所で低 pH を確認した．本研究ではこれを模擬した計算上の CO_2 漏出を推定した．逆時間方向計算は 0.3 s/step で 10 日分とした．漏出位置はセル番号で A(12, 12), B(14, 14)，開始時刻は τ_{seep} = 691200 sec，フラックスはともに 1×10^{-7} kg/m^3/s とした．計算領域の格子設定と水深（10 m 間隔の等高線），漏出位置 A, B と水平方向の観測位置と漏出点を含む鉛直断面での CO_2 分布を Fig. 7 に示す．x, y 方向に着目すると ΔL_M が d_S に等しいため，Fig. 6 に示した Group C から得られた知見より 2 漏出点の推定は可能だと考えられる．

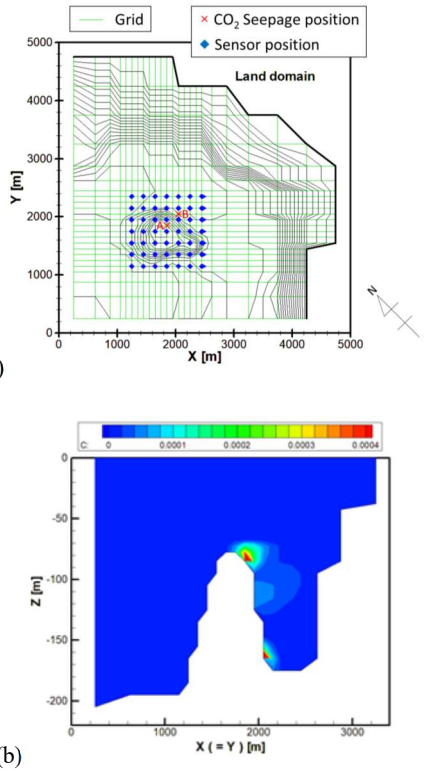

Fig. 7 (a) Two seepage positions and sensors and (b) CO_2 distribution on $x = y$ in 3D domain.

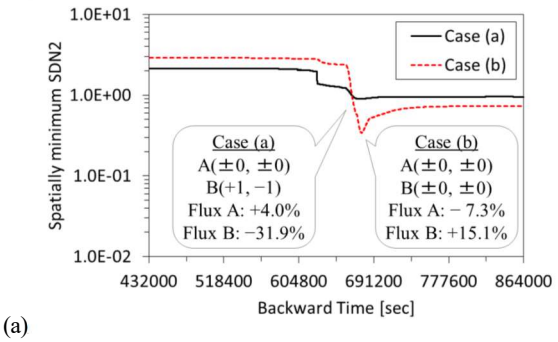

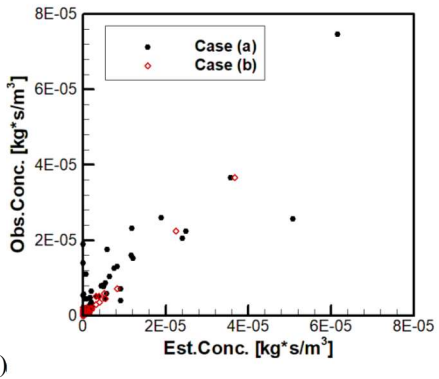

Fig. 8 (a) Time change of spatially minimum SDN2 and (b) Linear regression between measured and estimated CO_2 concentrations.

センサを深度 77.5 m と海底の両方に設置したとき，設置したセンサ全てを使用した場合を Case (a)，$m = 0.5$ として残差の大きな観測データを除外した場合を Case (b)とした．SDN2 の空間最小値の時間変化と推定位置と推定フラックスの誤差を Fig. 8(a) に，SDN2 の空間最小値の時間最小値を与える時間における推定位置における，各センサの観測濃度と推定濃度の線形回帰グラフを Fig. 8(b)に示す．Case (a)では推定位置 B が真の位置から x, y 方向に 1 セルずつずれ，観測データ点が一直線上に乗らなかったが，Case (b)では一致した．したがって $m = 0.5$ として残差の大きな観測データを除外することの有効性が示唆された．

5. 結論

本研究では海底下 CCS で想定される複数点 CO_2 漏出の推定手法を新たに開発し，本手法の使用に際しての知見と適用限界を，二次元テスト計算を通して無次元パラメタで定量的に表した．また，それを基に三次元計算を実施し，推定誤差の要因となる観測データの除外方法の有効性を示唆した．

文献

[1] 森千晶，佐藤徹，大山裕之 他：日本船舶海洋工学会論文集 26, 203–212 (2017).
[2] R. Sakaizawa, T. Sato, C. Mori et al., Journal of Greenhouse Gas Control 84, 131–146 (2019).
[3] 下島公紀：電力中央研究所報告 V09035 (2010).

Development of Estimation Method for Multiple Seepage Locations of Marine Pollutants

Project Representative
Toru Sato　Department of Ocean Technology, Policy, and Environment Graduate School, Graduate School of Frontier Sciences, The University of Tokyo

Authors
Shunsuke Kanao*[1], Toru Sato*[1], Alan Junji Yamaguchi*[1]
*[1] Department of Ocean Technology, Policy, and Environment Graduate School, Graduate School of Frontier Sciences, The University of Tokyo

When abnormally high concentration of a pollutant is observed in the ocean, it is necessary to search for seepage positions and fluxes of the pollutant. In this study, to reduce time and expense of such detection effort, we proposed a numerical method for estimating multiple seepage positions and fluxes using a limited number of observed concentration data. This method is called the adjoint marginal sensitivity method, which is a time-backward probabilistic method to estimate seepage positions and fluxes. We would like to emphasize that the proposed method can deal with multiple seepage points as its originality. In this study, we validated the newly developed method and showed the conditions for successful estimation using the simulation results of series of well-planned two-dimensional case studies where flow velocity, distance between two seepage positions, and spatial observation range were changed to investigate their effects on the estimation accuracy.

Keywords : Adjoint method; Marine hydrodynamics; Marginal sensitivity method; Marine pollutant; Multiple seepage locations

1. Introduction

In order to mitigate global warming, it is necessary to reduce CO_2 emissions into the atmosphere. Sub-seabed CO_2 Capture and Storage (CCS), by which CO_2 is separated and collected at emission sources such as power plants, and then injected and stored in reservoirs below the seabed, is attracting attention. Considering the possibility of CO_2 seepage into seawater, the sub-seabed CCS operators are obliged to monitor the CO_2 concentration in the sea under the Marine Pollution Control Act. If a high concentration is detected, it is necessary to conduct a re-investigation, which requires a large amount of cost and a long time. Therefore, it is very effective to numerically estimate the seep location while using the observed concentration data to narrow the re-investigation area and reduce the cost and required time. Mori et al. [1] and Sakaizawa et al. [2], who applied the Adjoint Marginal Sensitivity Method, as prior studies on estimations of seepage position, time, and volume under unsteady flow successfully. However, multiple seepage points were not taken into consideration. In reality, because seepage does not necessarily from a single position, this study aims to develop a method that can estimate seeps from multiple positions, and to show its application limits.

2. Method

2.1 Time-forward calculation

In order to obtain velocity data, we solve the Navier-Stokes equations (1)-(3) and continuity equation (4) under hydrostatic approximation. Where t is time, u, v and w are the flow velocities in the x, y and z directions, p is the pressure, ρ and ρ_0 are the density and the reference density, A_M and K_M are the horizontal and vertical eddy viscosity coefficients, and g is the gravitational acceleration, and f_{Cor} are the Coriolis parameter.

$$\frac{\partial u}{\partial t}+u\frac{\partial u}{\partial x}+v\frac{\partial u}{\partial y}+w\frac{\partial u}{\partial z}-f_{cor}v$$

$$=-\frac{1}{\rho_0}\frac{\partial p}{\partial x}+A_{\mathrm{M}}\left(\frac{\partial^2 u}{\partial x^2}+\frac{\partial^2 u}{\partial y^2}\right)+\frac{\partial}{\partial z}\left(K_{\mathrm{M}}\frac{\partial u}{\partial z}\right) \quad (1)$$

$$\frac{\partial v}{\partial t}+u\frac{\partial v}{\partial x}+v\frac{\partial v}{\partial y}+w\frac{\partial v}{\partial z}+f_{cor}u$$

$$=-\frac{1}{\rho_0}\frac{\partial p}{\partial y}+A_{\mathrm{M}}\left(\frac{\partial^2 v}{\partial x^2}+\frac{\partial^2 v}{\partial y^2}\right)+\frac{\partial}{\partial z}\left(K_{\mathrm{M}}\frac{\partial v}{\partial z}\right) \quad (2)$$

$$0=-\frac{1}{\rho_0}\frac{\partial p}{\partial z}-\frac{\rho}{\rho_0}g \quad (3)$$

$$\frac{\partial u}{\partial x}+\frac{\partial v}{\partial y}+\frac{\partial w}{\partial z}=0 \quad (4)$$

In this study, in order to investigate the effectiveness and usage of this method, CO_2 is advected and diffused by a time-forward numerical simulation. In Equation (5), C is the CO_2 concentration, S_C is the seepage term, and A_C and K_C are the horizontal and vertical eddy diffusion coefficients.

$$\frac{\partial C}{\partial t}+\frac{\partial(u_j C)}{\partial x_j}=\frac{\partial}{\partial x_j}\left(D_C\frac{\partial C}{\partial x_j}\right)+S_C+q_{\mathrm{in}}C_{\mathrm{in}}-q_{\mathrm{out}}C \quad (5)$$

2.2 Time-backward calculation

In the Adjoint Marginal Sensitivity Method applied in this study, adjoint probability ψ_n ($n = 1, ..., N$) is advected and diffused in the time-backward direction using the stored flow velocity data. Here N is the number of observation points.

$$\frac{\partial \psi^*}{\partial \tau} - u_j \frac{\partial \psi^*}{\partial x_j} = \frac{\partial}{\partial x_j}\left(D_C \frac{\partial \psi^*}{\partial x_j}\right) - q_{\mathrm{out}} \psi^*$$

$$+\Pi(\boldsymbol{x} - \boldsymbol{x}_{\mathrm{obs}}) \Pi'(\tau\,;\, \tau_{\mathrm{obs}} - \Delta\tau_{\mathrm{obs}}\,, \tau_{\mathrm{obs}}) \qquad (6)$$

where τ is the reverse time, x_{obs}, n, τ_{obs}, n are the position and backward time of each observation, and $\Pi(\boldsymbol{x})$ is a rectangular function that takes 1 when $\boldsymbol{x} = 0$ and 0 when $\boldsymbol{x} \neq 0$. The adjoint probability has the dimension of time. A volume flux of one-point seepage CO_2 f is estimated as

$$\bar{f} = \frac{\sum G_n \Psi_n}{\sum {\Psi_n}^2} \qquad (7)$$

$$G_n = \int_{t_{\mathrm{obs},n}}^{t_{\mathrm{obs},n}+\Delta t_{\mathrm{obs},n}} C_n\left(\boldsymbol{x}_{\mathrm{obs},n}\,, t\right) \mathrm{d}t \qquad (8)$$

$$\Psi_n = \frac{|\Delta x_{\mathrm{seep}}|}{|\Delta x_{\mathrm{obs},n}|} \int_{\tau_{\mathrm{seep}}-\Delta\tau_{\mathrm{seep}}}^{\tau_{\mathrm{seep}}} \psi_n^*\left(\boldsymbol{x}_{\mathrm{seep}}\,, \tau\right) \mathrm{d}\tau \qquad (9)$$

where f is a constant value, C_n is each observed concentration, Δt is the calculation time increment, x_{seep} is the seepage position, and τ_{seep} and $\Delta\tau_{seep}$ are the seepage start reverse time and seepage duration. In case of continuous CO_2 seepage, $\tau_{seep} - \Delta\tau_{seep} = 0$.

In the case of multiple point seepage, the observed concentration C_n is decomposed into the reaching concentrations C_{An} and C_{Bn} derived from the seepage points A and B, and the respective seepage fluxes f_A and f_B are similarly estimated, based on the principle of superposition regarding the CO_2 concentration. Since the reached concentration is unknown, erasing it leads to

$$\Psi_{n\mathrm{A}} f_{\mathrm{A}} + \Psi_{n\mathrm{B}} f_{\mathrm{B}} = G_n \qquad (10)$$

where $\Psi_{n\mathrm{A}}$ and $\Psi_{n\mathrm{B}}$ are the time-integrated values of Ψ_n at the seep points A and B. The estimated seepage flux, which is the least-squares solution of this simultaneous equation, is expressed by Eqs. (11) and (12), and the estimated seepage position/time is the position/time that minimizes the index SDN2 in Eq. (13). However, in order to simplify the problem, CO_2 seeps from multiple points at the same time.

$$\bar{f}_{\mathrm{A}} = \frac{(\sum G_n \Psi_{n\mathrm{A}})(\sum {\Psi_{n\mathrm{B}}}^2) - (\sum G_n \Psi_{n\mathrm{B}})(\sum \Psi_{n\mathrm{A}} \Psi_{n\mathrm{B}})}{(\sum {\Psi_{n\mathrm{A}}}^2)(\sum {\Psi_{n\mathrm{B}}}^2) - (\sum \Psi_{n\mathrm{A}} \Psi_{n\mathrm{B}})^2} \qquad (11)$$

$$\bar{f}_{\mathrm{B}} = \frac{(\sum G_n \Psi_{n\mathrm{B}})(\sum {\Psi_{n\mathrm{A}}}^2) - (\sum G_n \Psi_{n\mathrm{A}})(\sum \Psi_{n\mathrm{A}} \Psi_{n\mathrm{B}})}{(\sum {\Psi_{n\mathrm{A}}}^2)(\sum {\Psi_{n\mathrm{B}}}^2) - (\sum \Psi_{n\mathrm{A}} \Psi_{n\mathrm{B}})^2} \qquad (12)$$

$$\mathrm{SDN2} = \frac{\sqrt{\frac{1}{N}\sum_{n=1}^{N} \{G_n - (\Psi_{n\mathrm{A}} \bar{f}_{\mathrm{A}} + \Psi_{n\mathrm{B}} \bar{f}_{\mathrm{B}})\}^2}}{\frac{1}{N}\sum_{n=1}^{N} G_n}$$

$$= \frac{\sqrt{N \sum_{n=1}^{N} \{G_n - (\Psi_{n\mathrm{A}} \bar{f}_{\mathrm{A}} + \Psi_{n\mathrm{B}} \bar{f}_{\mathrm{B}})\}^2}}{\sum_{n=1}^{N} G_n} \qquad (13)$$

3. Estimation of two-point seepage in 2D test area

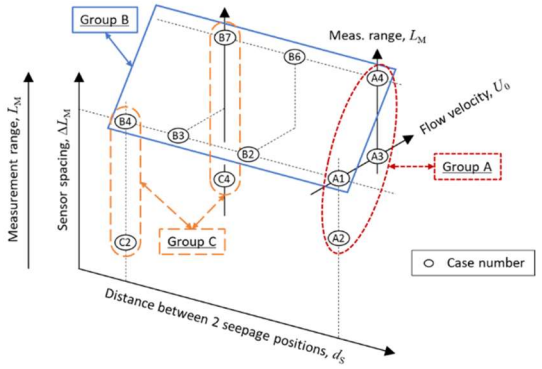

Fig. 1 Relationship among the cases for the two seepage point cases in Groups A, B, and C.

In this study, CO_2 was continuously seeped from the forward time t_{seep} = 51840 s (reverse time τ_{seep} = 120960 sec) under unsteady homogeneous flow in the 2D test area. The number of sensors is 16 and the eddy diffusion coefficient is fixed at D_C = 0.46 m^2/s. Then, the location and flux of the seepage were estimated by changing the width of the sensor installation range L_M (sensor interval ΔL_M), advection length $L_A = U_0 T_p / \pi$, distance between two seep points d_S,, the flux ratio r, and the offset of the sensor arrangement from the seepage positions. Figure 1 shows the relationship between each case. In Groups A to C, r = 1.

As an example, the seepage position at Case A1 (U_0 = 0.2 m/s), CO_2 distribution (t = 120960 sec), and the sensor arrangement are shown in Fig. 2, and the temporal change of spatially minimum SDN2 when Offset = 0 m is shown in Figure 3. SDN2 became the minimum near the seepage start time. Here, Re Sc = $L_A^2 / (D_C T_p)$ is a value on the order of 10^2. Figure 4 shows the relationship between L_M / L_A and the estimated position error when Offset = 0 m in Group A. From Group A, it can be seen that "L_M / L_A is about 1.7 or more" is required for accurate estimation of the two seepage positions.

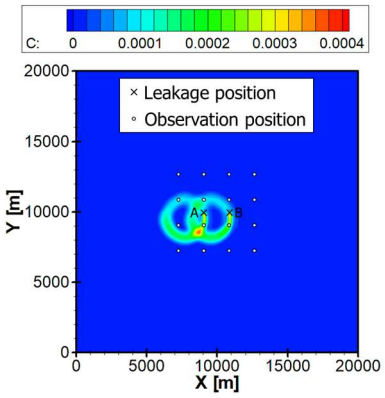

Fig. 2 Pollutant distribution at t = 129600 s and the observation positions in Case A1 for two seepage points.

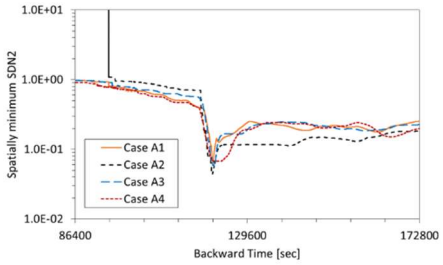

Fig. 3 Temporal change of the spatial minimum of SDN(2) in Group A for two seepage points.

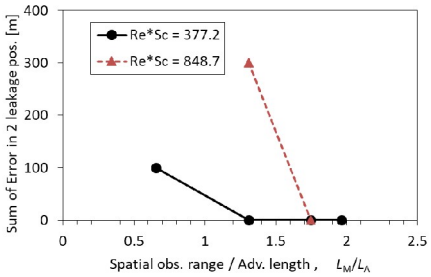

Fig. 4 Effect of nondimensional spatial observation range on estimated errors in seepage position in Group A for two seepage points.

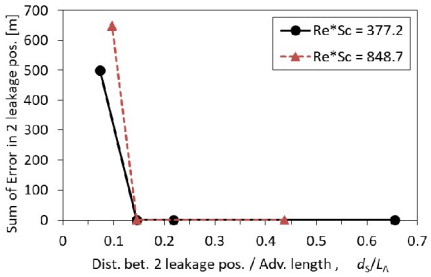

Fig. 5 Distance between two seepage positions and estimation error in them in Group B for two seepage points.

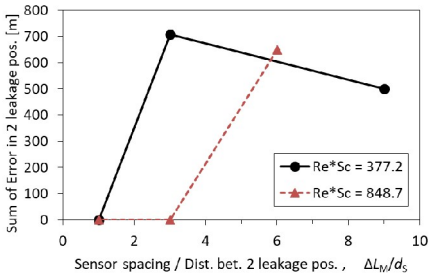

Fig. 6 Sensor spacing and estimation error in two seepage positions in Group C for two seepage points.

In Group B, d_S was made shorter than Cases A1 and A4 respectively. Figure 5 shows the relationship between d_S / L_A and the error in the estimated position when Offset = 0 m. It can be seen that the conditions shown in Group A hold when d_S / L_A is 0.15 or more. In Group C, the sensor interval was shortened from Cases B2 and B4 where d_S / L_A was less than 0.1. Figure 6 shows the relationship between $\Delta L_M / d_S$ and the error in the estimated position when Offset = 0 m. When d_S / L_A is 0.15 or less, "$\Delta L_M / d_S$ is about 1 or less" is effective.

4. Estimation of two-point seepage in a 3D test area simulating Kagoshima Bay

Shitashima [3] was confirmed two CO_2 seepage points near the top of the eastern slope of a seamount called Haorimushi site in the Kagoshima Bay. In this study, we tried to estimate these two seepage positions. The time-backward calculation was conducted for 10 days at a time step of 0.3 s. The seepage positions were set at A(12, 12) and B(14, 14), the seepage start time was τ_{seep} = 691200 s, and the flux was 1×10^{-7} kg/m^3/s. Figure 7 shows the horizontal grid setting of the computational domain, the water depth (contour lines at 10 m intervals), the seepage positions A and B, and the observation position in (a), and the seepage positions and seeping CO_2 distribution in the vertical section in (b). Since ΔL_M is equal to d_S, it is considered possible to estimate the two seepage points from the knowledge obtained from Group C shown in Fig. 6.

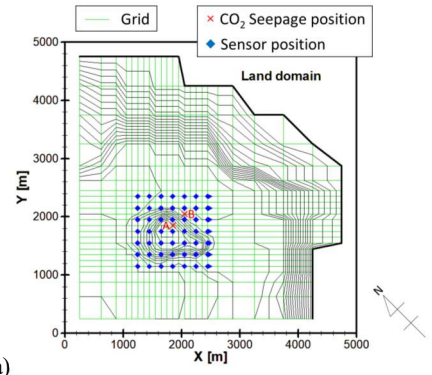

(a)

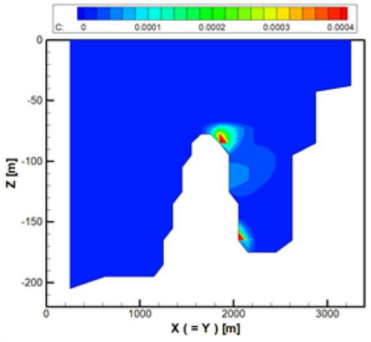

(b)

Fig. 7 (a) Two seepage positions and sensors and (b) CO_2 distribution on $x = y$ in 3D domain.

When the sensors were installed both at a depth of 77.5 m and the seabed, we set Case (a) as the case using all the installed sensors, and Case (b) as that excluding observation data with large residuals when m = 0.5. Figure 8(a) shows the time change of the spatial minimum of SDN2 and the estimation errors in the seepage positions and fluxes. In Case (a), the estimated position

B deviated from the true position by 1 cell (100 m) in the x and y directions. Figure 8(b) shows the linear regression between measured and estimated CO_2 concentrations at the estimated positions and at the temporal minimum of the spatial minimum of SDN2. In Case (a), the regression did not lie on a straight line, but in Case (b), it did. Therefore, it is recognized that excluding observation data with large residuals is effective when $m = 0.5$.

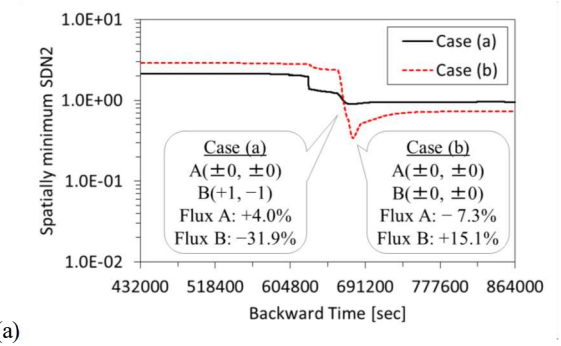

(a)

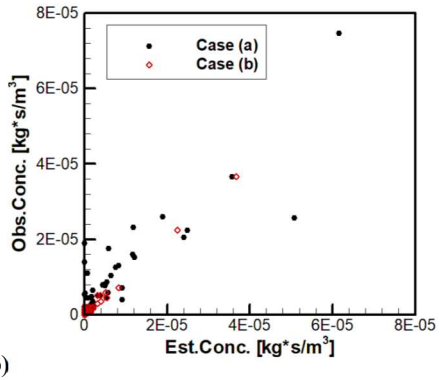

(b)

Fig. 8 (a) Time change of spatially minimum SDN2 and (b) Linear regression between measured and estimated CO_2 concentrations.

5. Conclusion

In this study, we newly developed a method for estimating multipoint CO_2 seepage that is assumed in sub-seabed CCS. Through 2D test calculations, quantitatively application limits quantitatively using dimensionless parameters. In addition, we performed 3D calculations and suggested the effectiveness of excluding the observation data with large deviations.

References

[1] Mori C, Sato T, Oyama H, Kano Y. (2017) J. Jpn. Soc. Naval Archit. Ocean Eng. 26 203–212 (in Japanese).
[2] Sakaizawa R, Sato T, Mori1 C, Oyama H, Tsumune D, Tsubono T, Kano Y. (2019) Int. J. Greenhouse Gas Control 84, 131–146.
[3] Shitashima K. (2010) CRIEPI Research Report V09034 (in Japanese).